

Comparative Fatigue Life Analysis on Flash Butt and Thermite Welds Using Durability and FE-Based Analysis

Thulani Sitimela¹, Siboniso Vilakazi², Leonard Msibi³, Johan van Aardt⁴
Transnet Freight Rail, Johannesburg, South Africa

ABSTRACT: Railway authorities utilise and rely on both exothermic and flash butt welding as joining methods for pearlitic rails during maintenance. The welding processes have been improved vastly over the years with the aim to ensure ease of execution and achieve better metallurgical properties. However, the Industrial Revolution 4.0 strategies for rail maintenance require more digitised and efficient weld management on track to prevent railway line closures and inherently assist in efficiency of operation. In this study, simulated thermite and flash butt welds using Finite Element method were analysed to determine fatigue life using the strain based module of nCode. The data obtained from load cells placed on the rail during passage of a loaded (100 wagon) 30 ton per axle train using strain gauges and linear variable differential transformers (LVDTs) was used as input to the fatigue model. A time series load was applied with a factor of 1.0. The resultant mechanical and metallurgical properties after welding for both flash butt and thermite welding were also incorporated into the FEA model. Thermite welds were found to have a lower fatigue life on the foot of the rail when the load factor was increased to 10. Thermite welds have wider HAZs which have depleted tensile properties and exhibit high localised plastic deformation. Rails joined using flash butt have more fatigue life cycles even with higher load factors indicating less possibility of fatigue crack initiation compared to exothermic welds.

1 INTRODUCTION

The railway system is one of the most efficient methods of transporting high volumes of goods and commodities. The system consists of steel beams of rail as the key infrastructure to provide a path for rolling stock to move on.

However, railway authorities are constantly challenged by rail break failures. The rail break types can be split into two categories:

- 1) Rail Flaw Related Rail Breaks
- 2) Welding Related Rail Breaks

Rail Flaw related rail breaks are defects that are detected using ultrasonic non-destructive testing method. Cracks (transverse, longitudinal or rolling contact fatigue) are one of the critical defects.

Welding related rail breaks occur mostly adjacent to or transverse through a welded joint. Rail breaks lead to increased frequency of maintenance, line occupation times, high maintenance cost and inherently loss of revenue.

Literature states that the main causes of failure in modern rails used for haulage are strain and stress as these control fatigue due to loading effected by a locomotives and its wagon wheels. It is further articulated that fatigue growth is facilitated by residual stress fields introduced during manufacturing and welding of rails. The highest tensile residual stress area is found at the web of the rail after cooling of welds [1] - [2].



Figure 1: Transverse failure adjacent to the weld

1.1 Rail Welding and Quality Control

Heavy Haul authorities utilize three welding methods to develop continuously welded rails (CWR). Flash butt, gas pressure and aluminothermic welding are the most commonly employed welding processes.

Flash butt is a resistance welding process consisting of electrical heating and hydraulic forging to join new rails together. The process is done mainly in stationery workshops and does not require filler material. [3]

Gas pressure welding is defined as a solid state welding process without additional filler material. This is achieved by application of significant axial pressure and heating of the joining area with an oxy-acetylene flame to temperatures ranging from 1100°C to 1300°C up to until upsetting values are reached. The welding processes has the ability to achieve similar strength values on the weld as that of the base metal. Gas welding process is flexible to both in plant and on track (field) welding [4].

Aluminothermic welding is a combination of casting and joining process which utilizes the Goldschmidt exothermic reaction to produce the molten steel. The thermite steel portion is the filler material which is casted as molten metal into the mould cavity. It is one of the most flexible and economic process chosen for field joining of new rails and also during maintenance when replacing or removal of defected rails. [5]

All the above mentioned welding methods yield suitable mechanical properties to sustain heavy haul loads. The standards used for qualification of the rail welding process in terms of its associated mechanical and metallurgical properties are BS EN 14730-1 and BS EN 14587-1 for aluminothermic and flash butt welding respectively. The most common properties of welds tested during qualification of laboratory test welds are; hardness (proportional to tensile strength), fatigue, deflection from slow bend tests, and susceptible macro and microstructure.

Hardness is the resistance of a material to plastic deformation, rail welds experience higher hardness compared to parent materials due to higher cooling rates during solidification. Harder welds fail in a brittle manner. Brittle fracture occurs as a result of uncontrolled and rapid crack growth, unlike ductile failure. Brittle fracture is the most preferred failure mode on rails, since little or no plastic deformation occurs. Plastic deformation on the rail results in rail expansion which in turn leads to kick-outs which have a potential to cause potential a derailment. Derailments may cause a severe loss of life, damage to the infrastructure and goods [3]. Bend tests are done using a three-point bend test to determine the extent of deflection and the minimum breaking load of a welded rail.

Different welded rail profiles have specified minimum breaking load and corresponding amount of deflection to be declared suitable to be installed on track. Macro structural analysis provides the welds soundness and measurements of the Heat Affected Zone (HAZ). Microscopic examination is done to evaluate the metallurgical phase transformation that occurred during the cooling of the welds against the continuous cooling curves or time-temperature transformation (TTT) diagrams. The modern high strength rail steel consists of the preferred pearlite phase which has good strength and has been improved over the years to increase its wear resistance.

The above mentioned properties ensure that the integrity of the rail welds is maintained during installation of welds on track.

1.2 The Heat Affected Zone (HAZ)

It is important to note that welded joints are microstructural discontinuities in rails [1]. During welding the so called Heat Affected Zone develops. The HAZ is the unmelted area adjacent to the weld which has its mechanical and metallurgical properties altered. This area is predominantly identified as the weakest point on the material after welding. Fundamentally, its formation is associated with globalised cementite (spherodised) which decreases the local yield and tensile strength of the HAZ. [1] - [6]

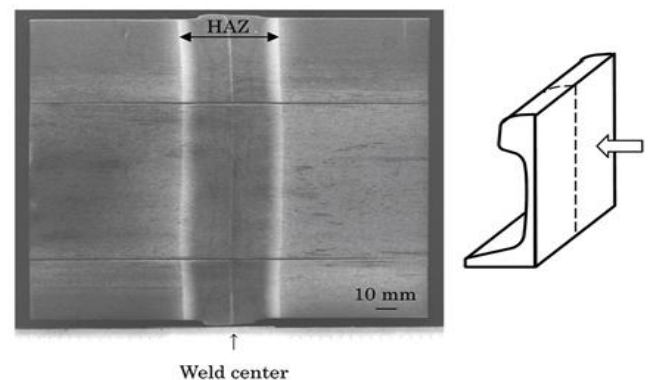


Figure 2: Typical HAZ in flash butt welded rails [22]

The HAZ in figure 2 is the most susceptible region to fatigue crack initiation and propagation under cyclic load. Cyclic loading is the application of fluctuating or repeated loads, stresses, strains, or stress intensities to locations on structural components. The length or size of the heat affected zone differs for each welding process. Parameters like the gap size of the weld also influence the length of the HAZ, particularly in aluminothermic welds [7]. Gas pressure and flash butt welding processes have narrower lengths of the HAZ. Aluminothermic welds have wider lengths of the HAZ due to high amount of super heat produced by the process during the exothermic reaction.

1.3 Weld Fatigue Failure in rails

Fatigue failure refers to the tendency of a material to catastrophically fracture or fail due to a progressive crack under cyclic loading [7]. The stress applied is below the ultimate tensile strength of the material. Fatigue failure occurs in three stages;

- Crack initiation in the areas of high stress concentration
- Stable crack growth or incremental crack propagation and,
- Rapid crack growth

Fatigue crack nucleation always nucleates in the zones associated with high plastic deformation. The cracks grow along the slip planes of materials oblique to the direction of maximum stress. The rate of crack growth is fairly slow [8] - [9].

Literature also states that most of the fatigue life in materials lies within the first stage [1]. Stable crack growth is associated with crack propagation perpendicular to the maximum tensile strength. This phase is represented by the linear relationship called the Paris' Law with the equation [9]:

$$\frac{da}{dN} = C\Delta K^m \quad (1)$$

Where m and C are material constants whereas ΔK is the stress intensity range [10]. Figure 3 depicts the fatigue phenomenon

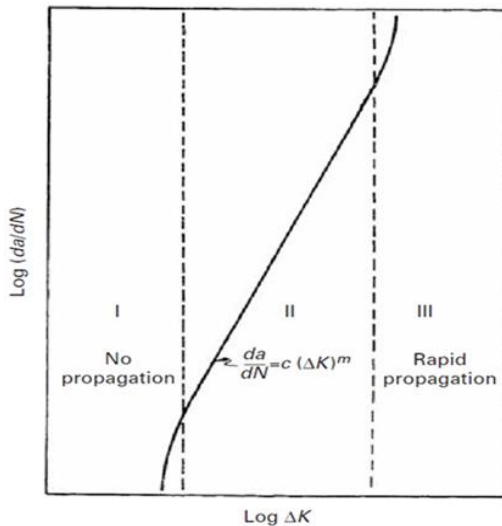


Figure 3: Typical fatigue crack growth curve [9]

Fatigue is further classified into Low Cycle and High Cycle fatigue. Low cycle fatigue (LCF) is strain based approach dependent on the local strain parameters. It is a thorough analysis on the local yielding at the stress concentrated areas during fatigue loading [10]. It is considered as a more accurate method of deriving fatigue lives. This is because it considers both local plastic deformation and employs local mean stress at the notch instead of the nominal stress on the component.

The Neuber's rule is used to obtain local strains at the notched areas by the Equation 2 (for elastic, perfectly plastic material beyond point of yielding [10]:

$$\epsilon_{\max,\min} = \frac{(K_t S_{\max,\min})^2}{E\sigma_y} \quad (2)$$

K_t is the stress concentration factor, S is stress range. The number of cycles to failure is determined using a strain life relationship (Coffin-Manson) for each value of amplitude strain. The total fatigue life is then determined using the damage accumulation rule by Palmgren-Miner [10] - [11].

High Cycle fatigue (HCF) is a stress based approach process. It is whereby repeated stresses in a member which are below ultimate tensile strength initially cause microscopic physical damage and failure on the component. Fatigue damage is directly based on the average nominal stresses in the affected area of the component [10]. According to EN 1993-1-9 the four main parameters that influence fatigue strength or resistance are;

- Stress range or loading type
- Structural detail geometry (track and joint)
- Material characteristics and,
- Environment

Fatigue life data (once the equivalent stresses are known) is represented in a so called Wohler curve which is a stress plots against the number of cycle to failure diagram (S-N Curve) [10]. A typical SN curve for ferrous and non-ferrous materials is shown in figure 4.

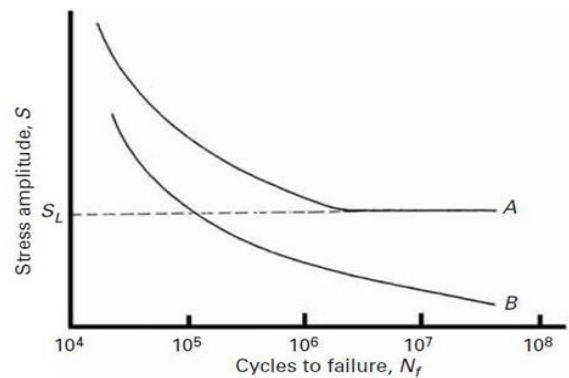


Figure 4: S-N curve for A ferrous, B non-ferrous material [9]

Fatigue crack growth and Paris Law are described by linear elastic fracture mechanics (LEFM) where a load is applied to a member containing an initial crack with certain crack length and the severity of growth is governed by the stress intensity factor (K_t) [10]. Therefore these will not be considered for this paper instead Low cycle fatigue (E-N analysis) or strain approach principles shall be utilised.

1.4 Case study

A macrofractographic analysis of reported rail breaks related to aluminothermic welding was studied over a period of four years. Fewer flash butt welds were recorded to have failed within the period. From field investigation, it was revealed that approximately over 50% of total weld related rail breaks occurred adjacent to the welds. The failure modes are similar to the image in Figure 1. The failure was assumed to have occurred predominantly in the HAZ (*see figure 1*). Laboratory failure analysis revealed that most of the welds failed transversely in a brittle manner. The fracture surfaces were associated with fatigue cracks located on the foot of the rails. Other factors were sharp edges at the weld collar, poor stripping of welds and geometrical misalignment. Crack initiation is intended to start in the high residual stress region (HAZ).

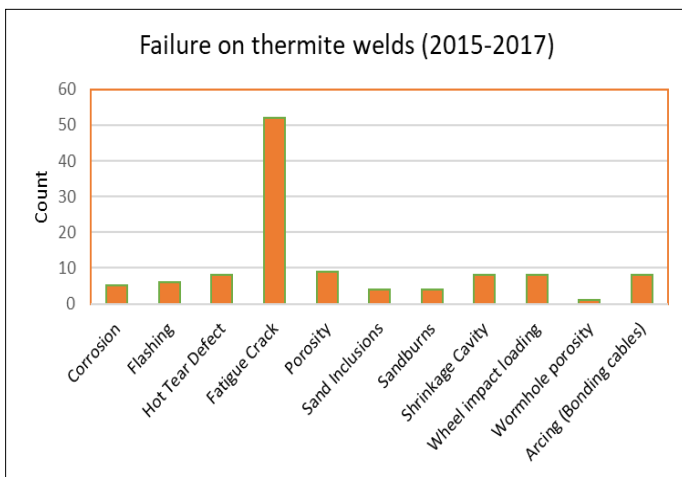


Figure 5: Root cause data from failure analysis of welding related rail breaks.

A similar study was conducted by L.B Godefroid et al, 2015 in an investigation of recurrent cases of fatigue fracture in flash butt welded rails. The author found that the cleavage facets on the rails were of brittle nature and the chevron marks were directed to a progressive fatigue crack on the rail foot. The area associated with concentric rings (dark area circled in Figure 6.) was identified as a high stress concentration region [1].

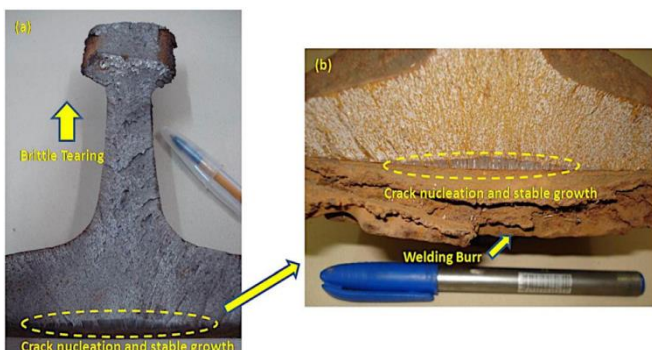


Figure 6: Fatigue crack at the rail foot [1]

Currently, various weld quality assessments methods are available to eradicate most of these weld related problems. The available non-destructive testing methods for welds (radiography) is only effective from a weld quality point of view. This is attributed by the fact that even welds that are defect free do fail predominantly in service and mainly as a result of fatigue cracks.

Rail welds continue to experience excessive and continuous bending moments about the neutral axis. The HAZ of welds is a site for high stress concentration because it is associated with high plastic deformation. Sites with high plastic deformation are prone to fatigue crack propagation. [11]

1.5 Laboratory Weld Fatigue Testing

The adopted standards governing laboratory testing scheme for fatigue life of rail weld on a flash butt and thermite welds are; BS EN 14587 and BS EN 14730-1 respectively [12] - [13]. Rail welds must achieve a minimum of 5×10^6 cycles under cycling loading with a load ratio of 0.1 and frequency of 10Hz.

The laboratory set up to conduct fatigue testing is shown below in Figure 7. It is a schematic of a rolling load test specified by AWS D15.2-94 specification.

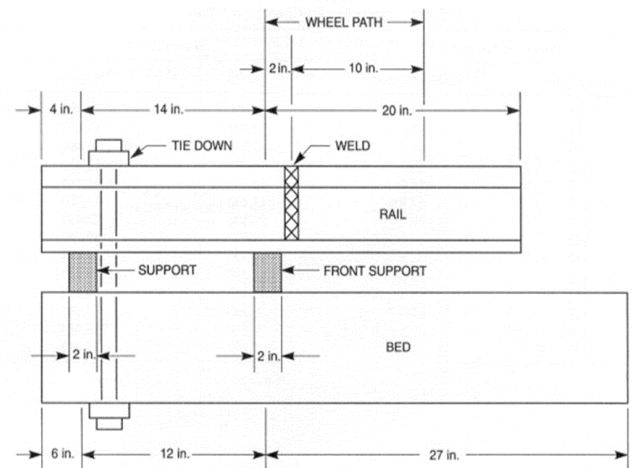


Figure 7: Rolling load test schematic as per AWS D15.2-94 [23]

The machine is a 4-point type bending machine and takes into account the entire weld geometry. The test speed or frequency of the machine shall be approximately 1 Hz or 60 cycles per minute for about 2 million cycles. The test does not individually access the effect of the HAZ on fatigue life. It determines the life of the entire weld combined with its HAZ.

In line with Industrial Revolution 4.0 key factors arise in providing digital solutions to reduce the frequency of maintenance or provide real time monitoring platforms on the railway infrastructure. The purpose of this paper is to indicate and provide comprehensive digital tools or a model to conduct Finite Element Analysis (FEA) and fatigue life calculation on aluminothermic and flash butt welds.

This model can be further incorporated in real time monitoring systems in the future. Comparisons between the two rail welding processes shall provide knowledge and idea of the type of maintenance interventions that the asset owner must take into consideration during infrastructure management.

Therefore, research and scientific simulations on fatigue life of rail welds gives practical insight to the asset manager on how to manage welds on track

2 MODEL GENERATION

Model assemblies for a flash butt welded rail and an aluminothermic welded rail on track are developed. A standard track parameters are considered for FEA and fatigue simulation for the two welding processes.

2.1 Contact Theory

The welded rails experience dynamic loading exerted by moving train wheels in service. Literature stated that the local stresses leading to fatigue crack growth are in the vicinity of the weld. Furthermore, these local stresses are effectively applied through wheel rail contact. The wheel rail contact phenomenon to be assumed for this study is that of Hertzian Contact.

The Hertzian contact theory expresses that when two elastic bodies are put together under loading, a contact patch exists on the surface in the form of an ellipse [14]. The effect of the residual stresses introduced by the welding processes as per figure 8 shall not be included in this simulation. The expected results of the simulation shall slightly differ from those obtained from the rolling load test since a static load will be assumed in the analysis.

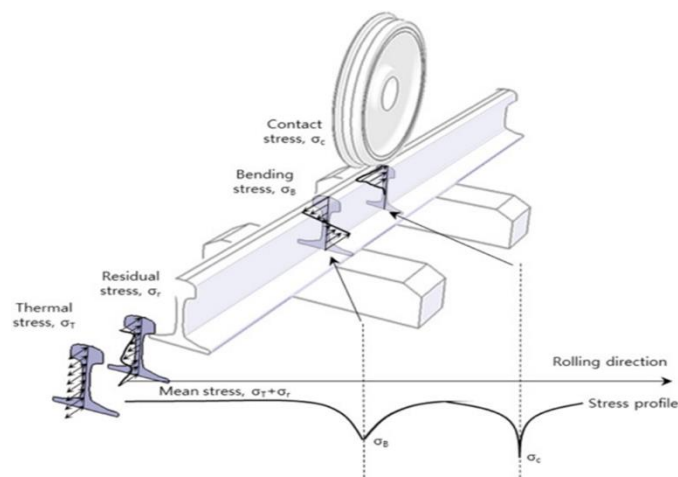


Figure 8: Schematic for wheel loading with residual stresses [30]

2.2 Materials Properties

The selected material properties for the parent rail, HAZ and the weld for a flash butt weld and aluminothermic weld were determined from laboratory quality analysis experiments. The tensile strength of the HAZ was determined from laboratory Vickers Hardness values. The values were converted to tensile stress using standard conversion charts. The properties considered in this context are in accordance with Transnet Freight Rail's Manual For Track Maintenance, BS EN 14730-1 and BS EN 13671-1 [12]-[13].

A welded 60E1, 350LHT rail profile at room temperature of 25°C is used. The rail's steel density is 7850kg/mm³. The Ultimate tensile strength (UTS) used is 1175 MPa with a modulus of elasticity of 205 GPa and 0.3 Poisson ratio is applied [12]. The approximated width of the HAZ was 10 mm and 25mm (for a 35 mm gap) for flash butt and thermite welds respectively. These will be included in the geometry.

The ultimate tensile strength of the HAZ was determined to range from 700-800 MPa and 850-950 MPa in thermite and flash butt welds, respectively. Furthermore, the tensile and compressive yield strengths (YS) used were estimated to range from 60-90% (UTS/YS ratio) of the respective tensile strength typical in carbon steels [15]. These properties will be assigned into the geometry.

2.3 Computer aided drawings (CAD)

The CAD model show below in figure 9 is a typical schematic or representative of the loading system of a locomotive or wagon wheel on track. However, static load application of the wheel in contact with the rail, weld and HAZ consecutively will be considered in determining the nominal stresses.

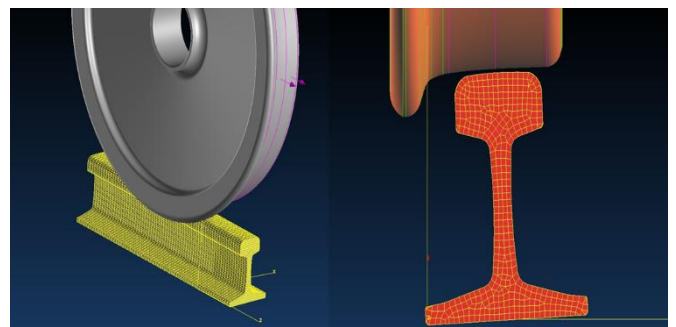


Figure 9: Wheel and the rail in contact

A simple geometry of an aluminothermic weld and its collar was assumed.

2.4 FEA and Boundary conditions

A 2-meter segment of rail was considered for this application and the rail ends were assumed to be symmetrical in the finite element application. A sleeper support system with approximately 650 mm spacing was used. The maximum contact stress was calculated using the Hertzian contact stress equation [14] - [15]:

$$P_o = \frac{1}{\pi} \left(\frac{6PE^2}{R^2} \right)^{\frac{1}{3}} \left(\frac{1}{F_1^2} \right) \quad (3)$$

Where R is the equivalent wheel radius of 780 mm and E is modulus of elasticity [15]. The factor $(1/F_1^2)$ accounts for ellipticity and was ignored. A single contact load case was assumed for the rail with the hertzian contact. The minimum contact pressure applied and determined using the equation above was approximately 1314.37MPa [16]. This was based on the load applied on a single leg of the rail used in this model.

The track static stiffness K considered was calculated using the equation since the track structure is characterised by material nonlinearity and geometrical nonlinearity [17]:

$$K = \left(\frac{P}{y} \right) \quad (4)$$

Where P is the load on the rail beam and y is the amount of deformation. [17]. Assuming an ideal track with vertical deformation of 2.5 mm the stiffness used was 58 860 N/mm.

A finite element analysis was conducted using Siemens NX¹ software on the two different types of welds. The solution used was that of non-linear static global constraints. A hexahedral mesh with uniform element size of 10 mm was used.

2.5 Fatigue Life Calculation

A fatigue life analysis software nCode² will be used calculate the nodal life of the rail with the two different welds. The software has inbuilt biaxial and three dimensional multiaxial assessment criterions. The finite element results, the equivalent von mises stresses and static bending results are used to determine;

- Fatigue life of the material
- Fatigue damage
- Fatigue factor of safety or design life

Strain gauge data obtained using from load cells is converted into a time series used as input data for the simulation. Load cells is a transducer that detects applied force and converts it into an electrical signal output that is proportional to the load. It consists of horizontal and vertical strain gauges used to measure the load exerted by a train passing a particular point over time. The loading phenomenon on track was measured using a 100 wagon fully loaded train at 30 tonnes per axle. The time series data was developed where the load will be applied with a scale factor of 1.0 and a frequency of 10Hz (see Figure 10).

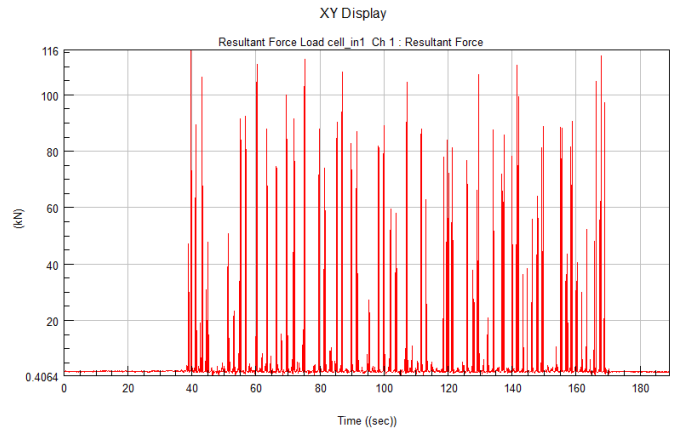


Figure 10: Time series data from strain gauge load cell transducers

An E-N Analysis glyph was used for the analysis. The E-N approach typically analyses local plastic deformation to determine total failure. The setup of the model is as shown in figure 11. The main inputs are FE model, material loading (strain gauge data) and material data or properties.

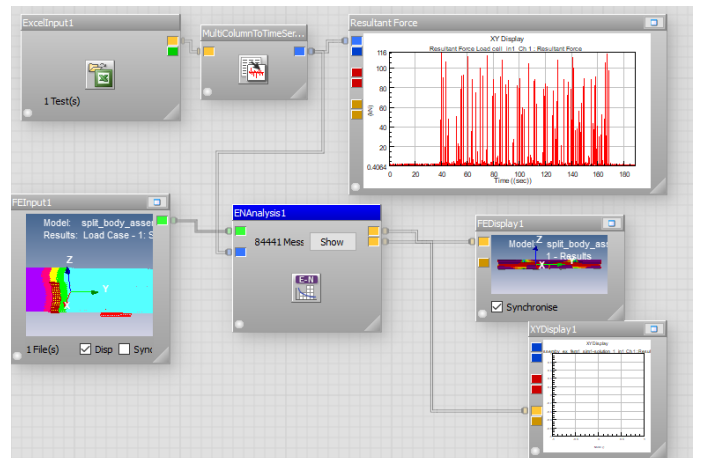


Figure 11: Setup of a fatigue EN analysis on nCode

¹ Siemens NX is a computer aided design software program with a built in FEA module.

² nCode is a software that provides a powerful range of solutions to process measured data, perform durability and FE-based fatigue analysis

The standard EN method (strain life) in nCode uses the Coffin-Manson-Basquin formula. It uses inbuilt multiaxial damage models namely Wang Brown with Mean models. The available mean stress correction models are Morrow and Smith Watson Topper. The Morrow correction method and Neuber plasticity correction is used for this model.

3 RESULTS AND DISCUSSIONS

3.1 FEA Results

The finite element results from rails joined using flash butt welding are shown in Figures 12-13. The static load was applied directly on the rail weld and the Equivalent von Mises and maximum Principal stresses were determined thereafter. Highest stresses were experienced on the contact area and on the foot of the rail where the highest bending moments occur.

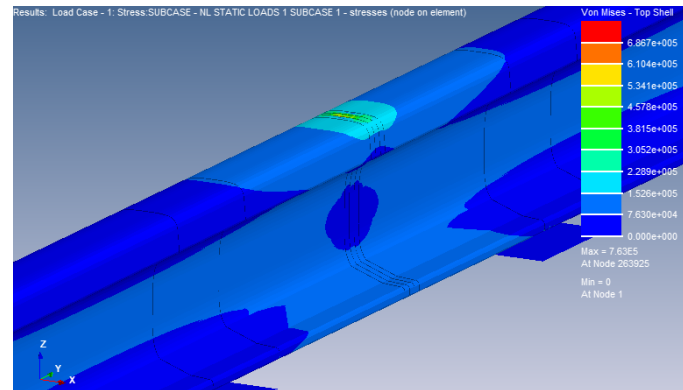


Figure 12: Von mises stress on a flash butt weld

Figure 13 reveals the effect of high bending moments experienced by a rail foot typical in beam structures.

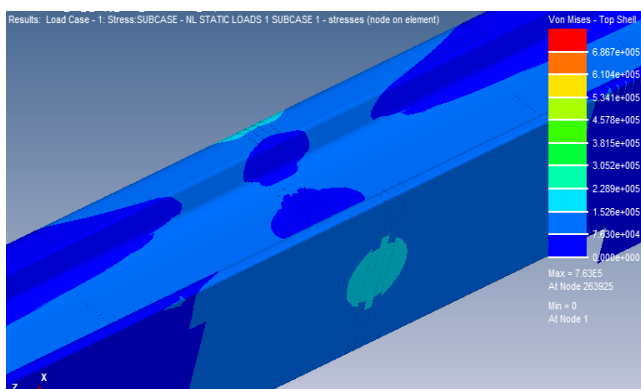


Figure 13: Von mises stresses on the foot (flash butt weld) showing site of highest bending stress

The FEA results for rails joined by the aluminothermic welding process are shown in Figures 14-15. The aluminothermic welds displayed regions of high stress concentration revealed by the higher magnitude of von Mises (MPa) on the weld (contact area) and foot area.

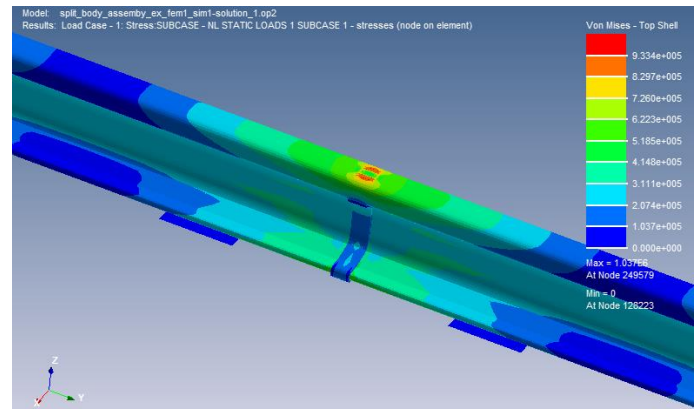


Figure 14: Von mises stress distribution in a thermite weld rail

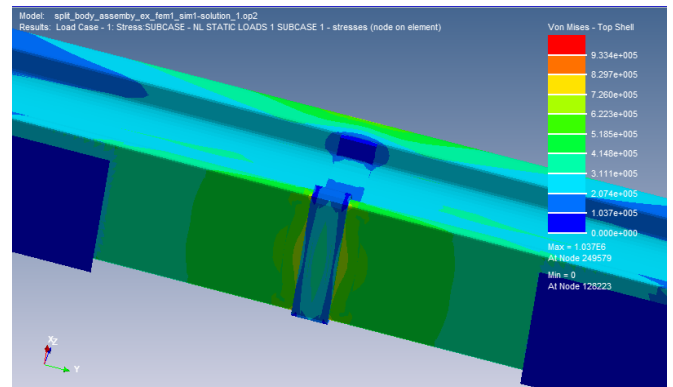


Figure 15: Von mises stress distribution on the foot of a thermite welded rail indicating high bending stresses

High equivalent stresses in the weld collar vicinity on the foot the rail in Figure 15 depicts a site for fatigue crack initiation. During loading the foot area experiences the highest bending stress whilst associated with weak material properties of a thermite weld. The weld collar edge also acts as a potential stress raiser.

The FEA results from figures 11-14 were used as inputs to calculate the fatigue life and damage on the regions of high stress concentration.

3.2 Fatigue Life

The fatigue life results from the simulation using nCode software for rails joined using the flash butt welding process are shown in figures 17-19. A time series input from strain gauge data in Figure 10 with a load factor of 1.0 was used. The outcome was unlimited number of cycles to failure. Furthermore the factor was increased to 10 times (see Figure 16) and still no fatigue damage was observed.

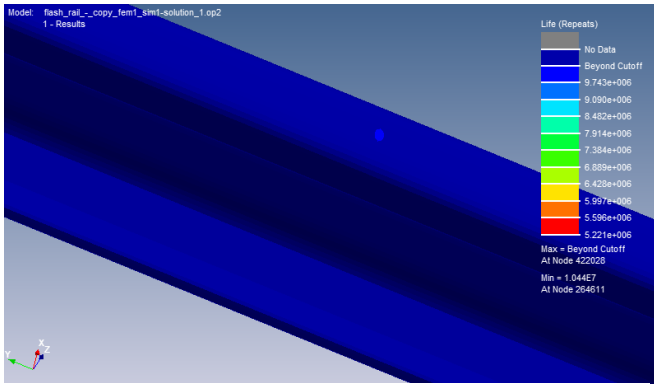


Figure 16: Fatigue life with load factor 10 in flash butt welded rail

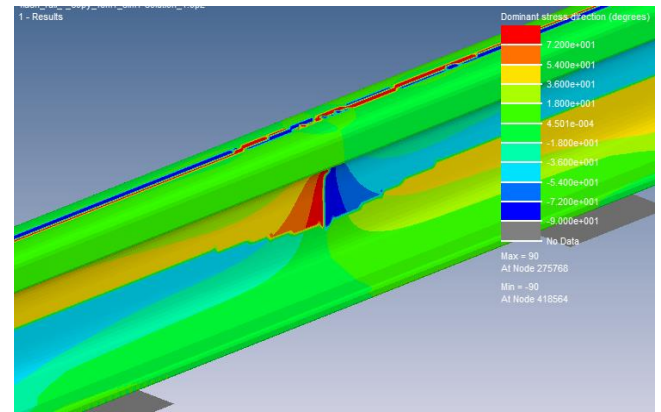


Figure 19: Biaxial stress direction in a flash butt welded rail with a load factor of 50

The load factor was then amplified to 50 times (see Figure 18) where significant fatigue results were observed. Fatigue damage was observed mainly in the contact area and on the foot of the rail. The foot of the rail is the most critical for initiation of fatigue cracks as indicated in literature.

The thermite welded joints (Figures 20-22) were analysed with load factor of 10. The fatigue life in thermite welds was lower compared to flash butt welds (analysed at 50 times load factor). The analysis was not done up to static failure. But the highest fatigue damage was observed on the foot and edge of the weld collar (stress raiser). This is because thermite welds have relatively wider HAZ with low tensile and yield strength values compared to flash butt welds.

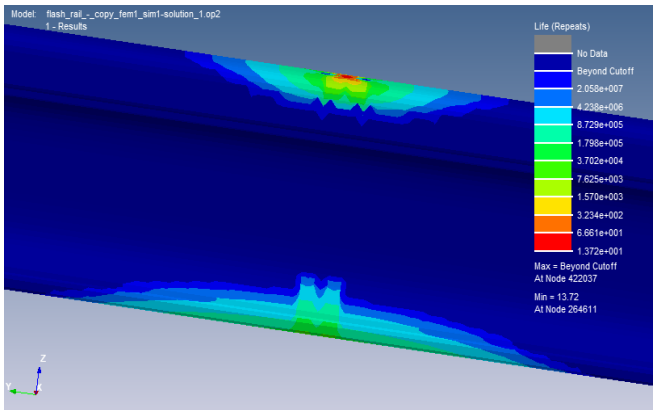


Figure 17: Fatigue life distribution at load factor 50 in a flash butt welded rail

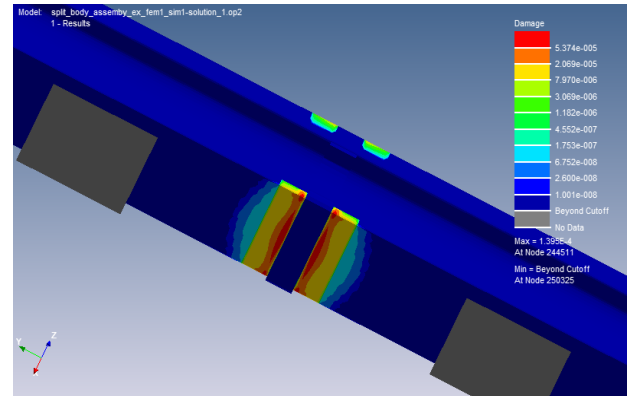


Figure 20: Regions with extreme fatigue damage in a thermite welded rail with a load factor 10

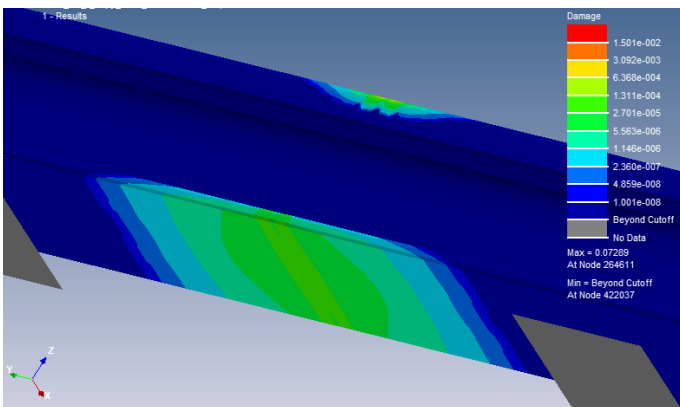


Figure 18: Fatigue damage on the foot of flash butt welded rail at load factor 50

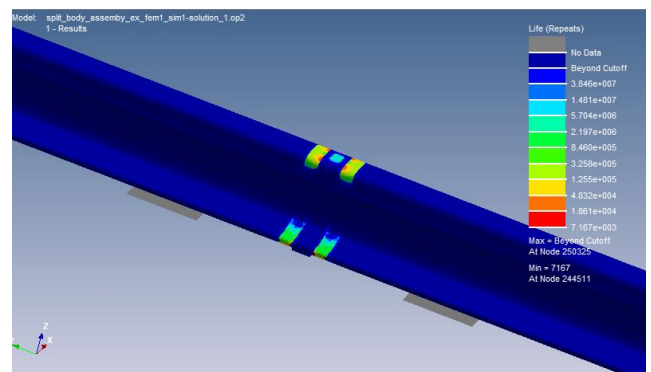


Figure 21: Fatigue life of a thermite welded rail at load factor 10

The low mechanical properties of the weld and HAZ of thermite welds results in the high localised plastic deformation as observed in FEA results. Hence thermite welds are expected to generate lower fatigue life values. Low fatigue life in the HAZ is observed in Figure 21 to reveal high localised plastic deformation. The HAZ in thermite welds is wider and has low tensile and compressive yield strength hence it is susceptible to deformation.

The biaxial stress direction values in figure 22 are similar to that in Figure 19 to confirm that loading profile was similar for both welded rails.

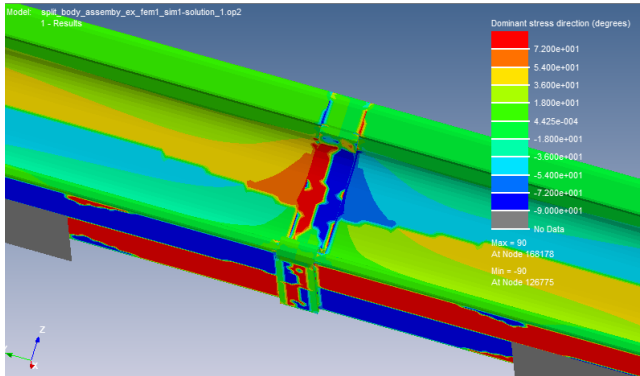


Figure 22: Biaxial stress direction in a thermite welded rail

4 CONCLUSIONS

Rail welds joined using the flash butt welding method have comparable narrower HAZ and inherently better mechanical properties than thermite welds. Thermite welds have a wider HAZ with reduced tensile properties and experience the highest stress concentration. The weld collar design on the foot of the rail in thermite welds is a potential stress raiser and is site for fatigue crack initiation. This is the region that experiences the highest localised bending moments during static and dynamic loading.

The FEA results from static loading reveal that all rail welds have the highest stresses in the HAZ on the foot. This was revealed by the highest equivalent and von mises stress distribution in the foot area. Flash butt welds subjected to similar loads as thermite welds exhibit a lower stress concentration and equivalent stresses because of its higher tensile properties.

Fatigue analysis results from nCode revealed that aluminothermic welds have poor resistance to fatigue crack initiation. Flash butt welded rails have over 5 times the life of an aluminothermic weld. Flash butt welded rails have almost similar properties to a rail segment without a weld. This is in line with the case study in section 1.4. The results obtained address the root cause (localised plastic deformation) compared to average results produced by a laboratory fatigue test.

5 RECOMMENDATIONS

Dynamic load finite element simulations are required to be conducted to take into account a more realistic approach. The effect of residual stresses stiffness must be considered for future work in order to yield correct results. The S-N and EN curves for the two welding processes must be developed through rainflow cycle counting in order to compare the fatigue life of the welding processes from an order of magnitude point of view. It is recommended for continuous development that the same simulation is done for a track with a low or high stiffness value to assess the effect of track parameters on fatigue life of welds.

Lastly, the fatigue life comparisons must be done up until static failure occurs. This will give an idea of the equivalent load factor and number of cycles required for the welds to fail.

6 ACKNOWLEDGMENTS

We would like to gratify the Transnet Freight Rail Technical journal team for making this possible. We would like extend further gratitude to Mulalo Nethononda, Thato Mahlatji and Rotondwa Ludzulu (Mechanical Engineers) for playing a pivotal role in development of the model.

7 REFERENCES

- [1] L. Godefroid, G. Faria, L. Cândido and T. Viana, "Failure analysis of recurrent cases of fatigue fracture in flash butt welded rails," *Engineering Failure Analysis*, vol. 58, pp. 407-416, 2015.
- [2] A. Skyttebol, "Continuous welded railway rails: Residual stress analyses, fatigue assessments and experiments. PHD thesis," Chalmers University of Technology, Goteborg, Sweden, 2004.
- [3] S. Rajanna, "Evaluation of Microstructural and Mechanical response of thermite welded rail," *International Journal of Innovative Research in Science, Engineering and Technology*, vol. 2, no. 9, pp. 4775-4782, 2013.
- [4] R. Yamamoto, M. Tatsumi, H. Itoh, Y. Terashita and Y. Yoshida, "Gas Pressure Welding Method of Rails by Mixed Gas of Hydrogen and Ethylene Gas," *Railway Technical Research Institute*, vol. 55, no. 1, pp. 39-45, 2014.
- [5] A. S. J. A. Z. Jilabi, *Welding of Rail Steel*, Manchester: University of Manchester, 2015.
- [6] F. Zhang, B. Lv, B. Hu and Y. Li, "Flash butt welding steel crossing and carbon steel

- rail,” *Materials Science Engineering A*, Vols. 454-455, pp. 288-292, 2007.
- [7] A. Skyttebol, B. Josefson and J. Ringsberg, “Fatigue crack growth in a welded rail under the influence of residual stresses,” *Engineering Fracture Mechanics*, vol. 72, pp. 271-285, 2005.
- [8] J. H. H. A. B. M. Rosler, *Mechanical Behaviour of Engineering Materials: Metals, Ceramics, Polymers, and Composites*, Berlin, Springer, 2007.
- [9] M. Meyers and C. Krishan, *Mechanical Behaviour of materials*, 2nd ed., New York: Cambridge University Press, 2009.
- [10] X. U. Roldan, *Toolbox for fatigue analysis of beam structures and its possible application to railways*, Sweden: Goteborg, 2007.
- [11] I. Salehi, A. Kapoor and P. Mutton, “Multi-axial fatigue analysis of aluminothermic rail welds under high axle load conditions,” *International Journal of Fatigue*, vol. 33, pp. 1324-1336, 2011.
- [12] C. Steimbregger, *Fatigue of Welded Structures*, Lulea: Lulea University of Technology, 2014.
- [13] J. Kelleher, D. Buttle, P. Mummery and P. Withers, “Residual Stress Mapping in railway rails,” *Material Science Forum*, Vols. 490-491, pp. 165-170, 2005.
- [14] BS EN 13674-1, *Railway Track Application-Track-Rail Part1: Vignole Rails 46kg/m and above*, BSI Standards Publications, 2011.
- [15] BS EN 14730-1, *Railway Application-Track-Aluminothermic welding of rails Part 1: Approval of welding processes*, BSI British Standards, 2006.
- [16] S. Iwnicki, *Handbook of Railway Vehicle Dynamics*, London New York: Taylor and Francis Group, 2006.
- [17] Bannister, A.C; Harrison, PL Dr; Martin, I.W; Webster, SE, “Structural Integrity Assessment Procedures for European Industry: SUB-TASK2.3: Yield stress/Tensile Stress ratio: Results of Experimental Programme,” British Steel plc, United Kingdom, 1999.
- [18] John Leeper, Roy Allen, *Guidelines to Best Practices for Heavy Haul Railway Operations- Management of the wheel and the rail Interface*, Virginia: International Heavy Haul Association (IHHA), 2015.
- [19] T. a. O. U. Telliskivi, “Contact Mechanics Analysis of Measured Wheel Rail Profiles using Finite Element Method,” *Journal Of Rail and Rapid Transit*, vol. 215, no. 2, pp. 65-72, 2001.
- [20] P. Wang, L. Wang, R. Chen, J. Xu, J. Xu and M. Gao, “Overview and outlook on railway track stiffness measurement,” *Journal Mod Transport*, vol. 24, no. 2, pp. 89-102, 2016.
- [21] M. U. T. Y. Kenji Saita, “Trends in Rail Welding Technologies and Our Future Approach,” Nippon Steel & Sumimoto Metal, 2013.
- [22] A. L. M. Saarna, “Rail and Rail Weld Testing,” in *4th International DAAAM Conference*, Tallim, Estonia, 2004.
- [23] A. Skyttebol and B. Josefson, “Numerical Simulation of flash butt welding of railway rails,” Graz Publishing, Graz University of Technology, Austria, 2004.
- [24] K. Ozakgul, F. Piroglu and O. Caglayan, “An experimental investigation on flash butt welded rails,” *Engineering Failure Analysis*, vol. 57, pp. 21-30, 2015.
- [25] I. Grossoni, P. Shackleton, Y. Bezin and J. Jaiswal, “Longitudinal rail weld geometry control and assessment criteria,” *Engineering Failure Analysis*, vol. 80, pp. 352-367, 2017.
- [26] Z. Zhang, B. Andrawes and J. R. Edwards, “Parametric study on the distribution of longitudinal load in railway track under dynamic wheel loading using finite element analysis,” *SSRG International Journal of Civil Engineering*, vol. 2, no. 5, pp. 28-41, 2015.
- [27] Various Authors, *Guidelines to Best Practices for Heavy Haul Operations-Infrastructure construction and Maintenance Issues*, Virginia: International Heavy Haul Association, 2009.
- [28] H.-K. Jun, J.-W. Seo, I.-S. Jeon, S.-H. Lee and Y.-S. Chang, “Fracture and Fatigue crack growth analyses on a weld-repaired railway line,” *Engineering Failure Analysis*, vol. 59, pp. 478-492, 2016.
- [29] Mapaila, L.T. ; Sitimela, T.M. ; Msibi, L.L., “Simulation of the thermite welding process using 3D casting software,” in *International Heavy Haul Association*, Cape Town, 2017.